

with the program SPECFIT V.2.10 (R. A. Binstead, A. D. Hungerbühler, Spectrum Software Associates, Chapel Hill, NC, 1997). This program performs global least-squares fits which, in fluorescence titrations, include the entire measured wavelength region (multiple wavelength analysis). In the  $^1\text{H}$  NMR titrations at constant concentration of the molecular rod ( $c(\text{rod}) \approx 0.1\text{--}0.2\text{ mM}$ ,  $c(\text{dendrophane}) \approx 0.05\text{--}1\text{ mM}$ ), the complexation-induced shifts of the steroid  $\text{CH}_3(18)$  and  $\text{CH}_3(19)$  resonances and the  $\text{CH}_3\text{CH}_2\text{O}$  resonances were evaluated. In the fluorescence titrations at constant concentration of the molecular rod ( $c(\text{rod}) \approx 0.01\text{--}0.02\text{ mM}$ ,  $c(\text{dendrophane}) = 0.005\text{--}0.8\text{ mM}$ ), the emission intensity of the rod decreased upon addition of dendrophane and the emission maxima of **4a/4b** at saturation binding shifted by 5–16 nm to higher energy.

- [20] a) H.-J. Schneider, *Angew. Chem.* **1991**, *103*, 1419–1439; *Angew. Chem. Int. Ed. Engl.* **1991**, *30*, 1417–1436; b) H.-J. Schneider, T. Shiestel, P. Zimmermann, *J. Am. Chem. Soc.* **1992**, *114*, 7698–7703.
- [21] Multiple evidence for 2:1 complexation by **4a/4b** was obtained: 1) An excellent fit of the fluorescence and/or  $^1\text{H}$  NMR titration data to the 2:1 binding model was obtained. 2) Job plots of fluorescence data showed clear maxima at  $x(\text{dendrophane}) \approx 0.66$  (see D. V. Naik, W. L. Paul, R. M. Threault, S. G. Schulman, *Anal. Chem.* **1975**, *47*, 267–270). 3) The complexation-induced shifts observed for the  $^1\text{H}$  NMR signals for  $\text{CH}_3(18)$  and  $\text{CH}_3(19)$  of the steroids in solutions of **4a** and **2** are compatible with formation of a 2:1 complex; that is, they are of similar magnitude to those observed for these resonances in the 1:1 complexes formed by testosterone (**11**) or the mono-steroid rods **18a** and **18b**.
- [22] Insight II program, V. 97.0, Molecular Simulations Inc., San Diego 1997.
- [23] Strong broadening of the resonances prevented the application of  $^1\text{H}$  NMR titrations to determine stabilities of the complexes formed by **4b**.

## Desolvation of a Novel Microporous Hydrogen-Bonded Framework: Characterization by In Situ Single-Crystal and Powder X-ray Diffraction\*\*

Cameron J. Kepert, Dusan Heseck, Paul D. Beer,\* and Matthew J. Rosseinsky\*

Attention has recently focused on the use of the hydrogen bond,<sup>[1]</sup> and also the coordinate bond,<sup>[2]</sup> in the controlled assembly of porous molecular frameworks. Studies into the guest exchange and catalytic properties<sup>[3]</sup> of these materials have led to a growing recognition of molecular frameworks as zeolite analogues, many retaining their structural integrity with desolvation or solvent exchange. Aware of these devel-

opments, and of the importance of redox centers to heterogeneous catalysis<sup>[4]</sup> and molecular recognition by electrochemical sensing,<sup>[5]</sup> we have synthesized an electrochemically active organic species suitable for forming novel extended molecular frameworks. Here we show how hydrogen bonding and  $\pi \cdots \pi$  nonbonding interactions can produce a microporous framework of this species linked to a transition metal complex. The material described displays remarkable flexibility, and undergoes significant structural rearrangements with desolvation to leave an empty-channel material that shows selectivity to guest sorption.

By making use of slow diffusion in aqueous silica gels, we have synthesized crystals incorporating the diprotonated, redox-active tetra(carboxyl)tetrathiafulvalene anion  $\text{H}_2(\text{TC-TTF})^{2-}$ , hexaaquacobalt(II) cations, and solvent water molecules.  $[\text{Co}(\text{H}_2\text{O})_6]\text{H}_2(\text{TC-TTF}) \cdot 2\text{H}_2\text{O}$  (**A**) consists of a three-dimensional hydrogen-bonded network of  $[\text{Co}(\text{H}_2\text{O})_6]^{2+}$  and  $\text{H}_2(\text{TC-TTF})^{2-}$  ions (Figure 1).<sup>[6]</sup> Short

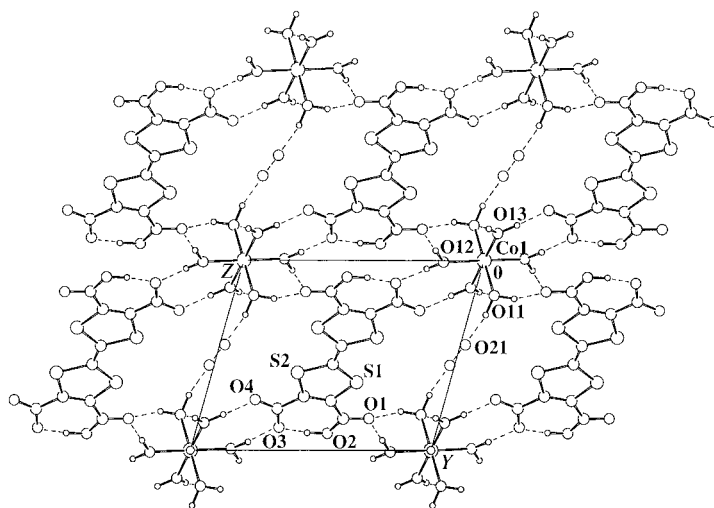


Figure 1. Projection of **A** down the  $a$  axis. For clarity, only one oxygen atom position of the disordered cavity water molecule is displayed. Selected bond lengths [Å] and angles [°] (a fixed value of 0.86 Å was used for O–H distances in the cation): O11  $\cdots$  O1\* 2.715(4), O12  $\cdots$  O3\* 2.773(4), O12  $\cdots$  O1\* 2.802(4), O13  $\cdots$  O4\* 2.685(4), O2  $\cdots$  O3 2.438(5), H2  $\cdots$  O3 1.47(8); O11–H11B  $\cdots$  O1\* 159(6), O12–H12B  $\cdots$  O3\* 173(8), O12–H12A  $\cdots$  O1\* 179(5), O13–H13A  $\cdots$  O4\* 174(6), O13–H13B  $\cdots$  O11\* 173(7), O3–H2  $\cdots$  O2 168(7).

hydrogen bonds exist between eight of the twelve protons in the hexaaquometal cation and six of the eight carboxyl oxygen atoms. The two protons of the doubly deprotonated acid form very short hydrogen bonds to neighboring carboxyl groups, giving this unit a rigid planarity. Running along the  $a$  axis, and lying parallel with slipped stacks of the TTF derivative and hydrogen-bonded chains of  $[\text{Co}(\text{H}_2\text{O})_6]^{2+}$  ions, are one-dimensional channels that are filled with zig-zag chains of disordered water molecules. The sites occupied by these molecules are defined by hydrogen bonding to the framework, primarily to a water molecule coordinated to  $\text{Co}^{2+}$  (O11) and to a lesser degree to O4 of the anion. Hydrogen bonding between solvent molecules occurs along the channels, the mean solvent separation being about 2.9 Å, compared with 2.8(1) Å for a typical hydrogen-bonded O  $\cdots$  O distance.

[\*] Dr. P. D. Beer, Dr. M. J. Rosseinsky, Dr. C. J. Kepert, Dr. D. Heseck  
Inorganic Chemistry Laboratory, Department of Chemistry  
University of Oxford  
South Parks Road, Oxford, OX1 3QR (UK)  
Fax: (+44) 1865-272-690  
E-mail: cameron.kepert@chem.ox.ac.uk  
paul.beer@chem.ox.ac.uk  
matthew.rosseinsky@chem.ox.ac.uk

[\*\*] C.J.K. thanks Christ Church, Oxford, for a Junior Research Fellowship. We thank Prof. C. K. Prout and Dr. D. J. Watkin for access to the X-ray diffractometer and for useful discussions.

Supporting information for this article is available on the WWW under <http://www.wiley-vch.de/home/angewandte/> or from the author.

A slight mismatching of this distance and the channel periodicity is a likely contributor to the solvent disorder.

Thermogravimetry reveals that the water molecules in the channels of **A** are liberated at 50 °C to leave [Co(H<sub>2</sub>O)<sub>6</sub>]H<sub>2</sub>(TC-TTF) (**B**). Four further equivalents of water are lost at 80 °C to provide polycrystalline [Co(H<sub>2</sub>O)<sub>2</sub>H<sub>2</sub>(TC-TTF)] (**C**),<sup>[7]</sup> in which the terminal carboxyl groups of the anion are thought to coordinate directly to the cobalt atom. Each of these desolvation steps leads to a considerable decrease in calculated density (see Table 1), with decreases in cell volume amounting to only about 8 Å<sup>3</sup> per liberated water molecule; the volume occupied by a typical solvent H<sub>2</sub>O molecule is 40 Å<sup>3</sup>.<sup>[8]</sup> The two remaining equivalents of water of **C** are lost above 120 °C, and decomposition occurs above 150 °C. The phases **A**–**C**, like other highly stable framework materials, are insoluble in a large range of common solvents (including water, alcohols, acetone, acetonitrile, carbon disulfide, and dichloromethane). Powder X-ray diffraction<sup>[7]</sup> indicates that **B** converts back into **A** upon rehydration at ambient temperature, whereas **C** transforms to a new crystalline form.

Remarkably, monocrystallinity is retained throughout the transition from **A** to **B**, allowing structure determination of **B** by single-crystal X-ray diffraction (Figure 2).<sup>[6]</sup> To our knowledge, this is the first time that such a study has been

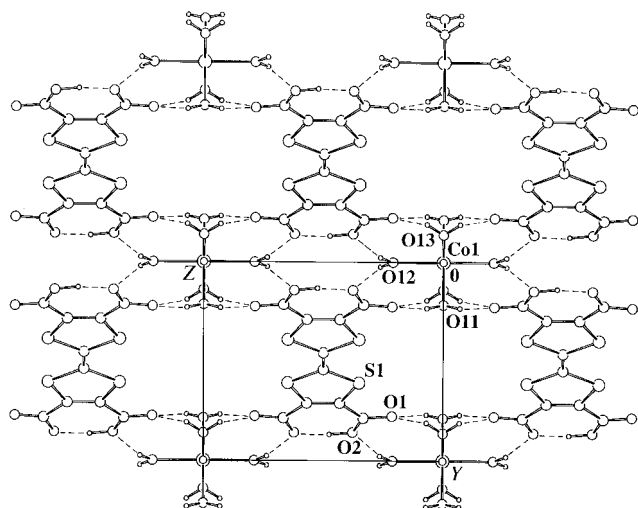


Figure 2. Projection of **B** (295 K) down the *a* axis. Note the retention of the one-dimensional channels from **A** upon desolvation. Selected lengths [Å]: O11...O1\* 2.897(14), O12...O2\* 2.812(11), O13...O1\* 2.727(12), O2...O2\* 2.421(17).

performed on an organic-based molecular framework material. Desolvation causes a considerable transformation of the unit cell, and an increase from triclinic to monoclinic symmetry (Table 1). Accordingly, the crystal morphology undergoes striking changes, in particular the adoption of a rectangular facet for the large (010) face and a considerable lengthening of the platelets. With the removal of the water molecules in the channel there are significant rotations of both cation and anion species, and both sites increase in symmetry from  $\bar{1}$  to 2/*m*. The driving force of the rearrangement is the formation of new hydrogen bonds as both cationic and anionic components cross-link to form the new frame-

Table 1. Unit cell parameters, formula masses, and calculated densities of **A**, **A'**, **B'**, **B**, and **C** at 295(2) K. **A'** and **B'** are intermediate, partially hydrated phases observed in situ during the **B** → **A** resolution.

	<b>A</b> <sup>[6, 7]</sup>	<b>A'</b> <sup>[7]</sup>	<b>B'</b> <sup>[7]</sup>	<b>B</b> <sup>[6, 7]</sup>	<b>C</b> <sup>[7]</sup>
<i>a</i> [Å]	5.239(1)	5.232(6)	6.426(2)	6.429(1)	6.956(4)
<i>b</i> [Å]	9.186(2)	9.134(17)	8.102(2)	8.079(2)	8.067(7)
<i>c</i> [Å]	11.749(3)	11.780(14)	9.915(4)	9.893(3)	9.063(8)
$\alpha$ [°]	74.158(11)	74.67(9)	90.0	90.0	80.51(3)
$\beta$ [°]	76.737(12)	76.78(6)	90.0	90.0	104.92(6)
$\gamma$ [°]	89.335(13)	89.29(10)	86.99(2)	86.76(2)	84.10(5)
<i>V</i> [Å <sup>3</sup> ]	528.7(2)	528.2(14)	515.3(3)	513.0(2)	479.0(6)
<i>M</i> [g mol <sup>-1</sup> ]	581.42	–	–	545.39	473.33
$\rho_{\text{calcd}}$ [Mg m <sup>-3</sup> ]	1.826	–	–	1.765	1.641

work: In **B**, each hexaaquo cation makes twelve rather than ten framework-forming hydrogen bonds, with four new cation–anion bonds replacing the two cation–cation and the two cation–solvent bonds. The stacks of H<sub>2</sub>(TC-TTF)<sup>2-</sup> undergo a considerable tilting from 45.1 to 33.3° with respect to the *a* axis, which is made possible by the presence of nonbonding  $\pi \cdots \pi$  interactions between anions (Figure 3).

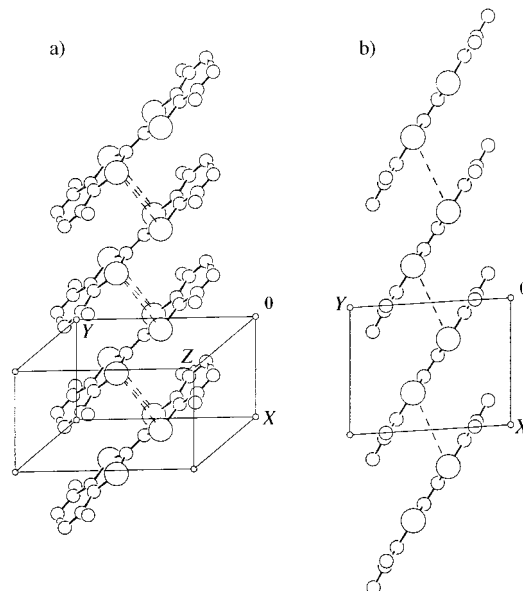


Figure 3. Projection of the one-dimensional stacks of H<sub>2</sub>(TC-TTF)<sup>2-</sup> in **A** (a) and **B** (b), drawn perpendicular to the *a* axis and on the same scale. Selected bond lengths [Å] in **A**: S1...S1\* 3.824(3), S1...S2\* 3.737(2); in **B**: S1...S1\* 4.115(7), 4.374(6).

These changes accompany a reduction in cross-sectional dimensions of the pseudo-rectangular channels within the framework: The width decreases from about 9 to 8 Å, and the height from 7 to 5 Å. Accordingly, the channels diminish in volume from about 62 Å<sup>3</sup> (12 % of the crystal volume) to about 41 Å<sup>3</sup> (8 %) per unit cell,<sup>[8]</sup> despite lengthening by 23 %.

In situ X-ray diffraction measurements<sup>[7]</sup> indicate that the resolution transition **B** → **A** occurs homogeneously over a powdered sample, and involves a gradual expansion in volume towards a maximally hydrated phase of **B** (**B'**) followed by a structural transition to a minimally hydrated phase of **A** (**A'**; see Table 1). Further rehydration returns **A'** to **A**. The robustness of the crystals suggests these structural rearrangements follow a pathway of very low energy, with inhomogeneities in the distribution of channel water molecules

apparently causing insufficient strain to produce fracturing. The observation that the **B** phase is capable of both containing and transporting water molecules within its channels is in accord with calculations on the minimization of the energy of inclusion,<sup>[9]</sup> which suggest that water sites within **B** have similarly low energies to those within **A**. The **B** → **A** structural transition is therefore likely to be governed primarily by a balance of hydrogen-bond energies, high levels of channel hydration favoring the existence of cation–solvent bonds as seen in **A**, and low levels favoring the enhanced framework hydrogen bonding of **B**.

The empty channel structure of **B** shows a high degree of selectivity towards guest sorption. Powder X-ray diffraction shows that samples of **B** exposed to methanol vapor at room temperature convert into a new crystalline form, whereas samples exposed to ethanol, carbon disulfide, and acetonitrile vapor remain unchanged over periods exceeding one month. These observations suggest that small polar molecules may readily be included into the empty channels, whereas larger or less polar molecules are excluded.

Compound **A** consists of a three-dimensional framework of transition metal centers and redox-active tetrathiafulvalene species which houses one-dimensional channels occupied by exchangeable water molecules. The assembly of hydrogen-bonding components can interact in a switchable fashion both with each other and with guest species, allowing the framework topology to alter smoothly and reversibly in response to a guest. We attribute the remarkable flexibility and durability of this unique microporous framework material to the multitude of independent weak (hydrogen bond) or nonbonding ( $\pi \cdots \pi$ ) intermolecular interactions present, meaning that bond breakage and formation energies are smaller than crystal fracturing energies. Importantly, the similarity in energies for interactions within the framework and between the framework and solvent molecules means that solvent inclusion may drastically affect the overall lattice energy, thereby providing a strong driving force for molecular rearrangement.

### Experimental Section

Tetrathiafulvalenetetracarboxylic acid,  $H_4(TC-TTF)$ , was synthesized according to literature methods.<sup>[10]</sup> Slow diffusion of  $H_4(TC-TTF)$  with 0, 2, and 4 parts of NaOH in aqueous silica gels afforded **A** on reaction with  $[Co^{II}(NO_3)_2] \cdot 6H_2O$  (aq).

Cyclic voltammetry:  $H_4(TC-TTF)$  (aqueous,  $0.5 \text{ mmol L}^{-1}$ ) undergoes a reversible one-electron oxidation at 0.58 V versus the standard mercury/calomel electrode ( $3.5 \text{ mol L}^{-1}$  KCl).

Received: April 14, 1998

Revised version: August 3, 1998 [Z 11721 IE]

German version: *Angew. Chem.* **1998**, *110*, 3335–3337

**Keywords:** crystal engineering • hydrogen bonds • microporosity • redox chemistry • tetrathiafulvalene

- [1] a) P. Brunet, M. Simard, J. D. Wuest, *J. Am. Chem. Soc.* **1997**, *119*, 2737–2738; b) K. Endo, T. Sawaki, M. Koyanagi, K. Kobayashi, H. Masuda, Y. Aoyama, *J. Am. Chem. Soc.* **1995**, *117*, 8341–8352; c) A. R. A. Palmans, J. A. J. M. Vekemans, H. Kooijman, A. L. Spek, E. W. Meijer, *Chem. Commun.* **1997**, 2247–2248; d) Y. Aoyama, K. Endo, T. Anzai, Y. Yamaguchi, T. Sawaki, K. Kobayashi, N. Kanehisa, H. Hashimoto, Y. Kai, H. Masuda, *J. Am. Chem. Soc.* **1996**, *118*, 5562–5571.

- [2] a) C. J. Kepert, M. J. Rosseinsky, *Chem. Commun.* **1998**, 31–32; b) O. M. Yaghi, C. E. Davis, G. M. Li, H. L. Li, *J. Am. Chem. Soc.* **1997**, *119*, 2861–2868; c) M. J. Plater, A. J. Roberts, R. A. Howie, *Chem. Commun.* **1997**, 893–894; d) D. L. Lohse, S. C. Sevov, *Angew. Chem.* **1997**, *109*, 1692–1695; *Angew. Chem. Int. Ed. Engl.* **1997**, *36*, 1619–1621; e) S. O. H. Gutschke, M. Molinier, A. K. Powell, P. T. Wood, *Angew. Chem.* **1997**, *109*, 1028–1029; *Angew. Chem. Int. Ed. Engl.* **1997**, *36*, 991–992; f) G. B. Gardner, D. Venkataraman, J. S. Moore, S. Lee, *Nature* **1995**, *374*, 792–795; g) S. R. Batten, B. F. Hoskins, R. Robson, *J. Am. Chem. Soc.* **1995**, *117*, 5385–5386; h) O. M. Yaghi, G. M. Li, H. L. Li, *Nature* **1995**, *378*, 703–706; i) D. Venkataraman, G. B. Gardner, S. Lee, J. S. Moore, *J. Am. Chem. Soc.* **1995**, *117*, 11600–11601; j) B. F. Abrahams, B. F. Hoskins, D. M. Michail, R. Robson, *Nature* **1994**, *369*, 727–729; k) C. Robl, *Mat. Res. Bull.* **1992**, *27*, 99–107.
- [3] a) K. Endo, T. Koike, T. Sawaki, O. Hayashida, H. Masuda, Y. Aoyama, *J. Am. Chem. Soc.* **1997**, *119*, 4117–4122; b) M. Fujita, Y. J. Kwon, S. Washizu, K. Ogura, *J. Am. Chem. Soc.* **1994**, *116*, 1151–1152.
- [4] a) I. W. C. E. Arends, R. A. Sheldon, M. Wallau, U. Schuchardt, *Angew. Chem.* **1997**, *109*, 1190–1211; *Angew. Chem. Int. Ed. Engl.* **1997**, *36*, 1144–1163; b) J. A. Dumesic, W. S. Millman, *ACS Symposium Series* **1990**, *437*, 66–74.
- [5] P. D. Beer, D. K. Smith, *Prog. Inorg. Chem.* **1997**, *46*, 1–96; C. Valerio, J. L. Fillaut, J. Ruiz, J. Guittard, J. C. Blais, D. Astruc, *J. Am. Chem. Soc.* **1997**, *119*, 2588–2589; P. D. Beer, *Chem. Commun.* **1996**, 689–696.
- [6] Single crystals of **A** were placed in open-ended capillaries on an Enraf-Nonius DIP2000 diffractometer equipped with Eu/Ba image plates and a nitrogen cryostream. To form **B**, a crystal of **A** was heated at  $10 \text{ K h}^{-1}$  to 328(2) K, then cooled at  $150 \text{ K h}^{-1}$  to 295(2) K. Crystal data for **A**:  $C_{10}H_{18}CoO_{16}S_4$ , triclinic, space group  $P\bar{1}$ ,  $F(000) = 297$ ,  $\lambda(\text{MoK}\alpha) = 0.71073 \text{ \AA}$ ,  $\mu(\text{MoK}\alpha) = 1.283 \text{ mm}^{-1}$ , crystal dimensions  $0.45 \times 0.30 \times 0.08 \text{ mm}$ ,  $2\theta_{\text{max}} = 53.26^\circ$ ,  $T = 295(2) \text{ K}$ , mosaicity =  $1.0^\circ$ . Crystal data for **B** at  $T = 295(2) \text{ K}$  and  $328(2) \text{ K}$ , respectively:  $C_{10}H_{14}CoO_{14}S_4$ , monoclinic, space group  $P112/m$ ,  $F(000) = 277$ ,  $\mu(\text{MoK}\alpha) = 1.309$  and  $1.313 \text{ mm}^{-1}$ , crystal dimension  $0.50 \times 0.20 \times 0.04 \text{ mm}$ ,  $2\theta_{\text{max}} = 53.44$  and  $53.50^\circ$ , mosaicity =  $1.0^\circ$ . Data reduction was carried out with the HKL suite of programs.<sup>[11]</sup> The structures were solved and refined with SHELXS-86 and SHELXL-93.<sup>[12]</sup> For **A**, **B** (295 K), and **B** (328 K), respectively, full-matrix least-squares refinement on  $F_o^2$  for 2057, 1080, and 934 unique data (4011, 2889, and 1684 collected reflections;  $R(\text{int}) = 0.034, 0.101$ , and  $0.109$ ); 182, 87, and 86 parameters; and 16, 41, and 41 restraints converged to  $wR2 = 0.1144, 0.2988$ , and  $0.3034$  (all data);  $R = 0.0651, 0.1686$ , and  $0.1783$  (1885, 954, and 779 data with  $F_o > 4\sigma(F_o)$ ); max./min. residual electron density  $0.511/-0.385, 1.610/-1.146$ , and  $0.807/-0.945 \text{ e \AA}^{-3}$ . Crystallographic data (excluding structure factors) for the structure(s) reported in this paper have been deposited with the Cambridge Crystallographic Data Centre as supplementary publication no. CCDC-101357. Copies of the data can be obtained free of charge on application to CCDC, 12 Union Road, Cambridge CB21EZ, UK (fax: (+44) 1223-336-033; e-mail: deposit@ccdc.cam.ac.uk).
- [7] Ground samples were sealed in 0.5-mm capillaries on a Siemens D5000 X-ray powder diffractometer with monochromated  $\text{CuK}\alpha_1$  radiation and a linear position-sensitive detector ( $6^\circ$ ). Gradual rehydration of **B** was achieved over a period of five days through an open-ended capillary packed with glass wool; no peak broadening was observed.
- [8] Channel volumes were calculated by summing voxels more than  $1.2 \text{ \AA}$  from the van der Waals surface of the host: A. L. Spek, *Acta Crystallogr. Sect. A* **1990**, *46*, 194–201.
- [9] Molecular docking using both CVFF and CFF91 atomic force fields: *Solids Docking 7.0, InsightII, Version 4.0.0*, Biosym Technologies, San Diego, CA, **1997**.
- [10] S. Yoneda, T. Kawase, M. Inaba, Z. Yoshida, *J. Org. Chem.* **1978**, *43*(4), 595–598.
- [11] Z. Otwinowski, W. Minor in *Methods in Enzymology* (Eds.: C. W. Carter, R. M. Sweet), Academic Press, New York, **1996**, p. 276.
- [12] G. M. Sheldrick, *SHELXS-86* and *SHELXL-93*, Universität Göttingen.